Factors Influencing Magnetic Protein Nanospheres Prepared by Sonochemical Method

Xiaojuan Zhang,[1] Dan Song,[2] Wei Jiang,[3] Zhendong Sun,[3] Lingyun Hao,[1] Yuanfeng Ye,[1] Xiaoli Yang,[1] Xiaohong Hu,[1] Fengsheng Li[3]

[1]*School of Material Engineering, Jinling Institute of Technology, Nanjing 211169, China*
[2]*China Research and Development Academy of Machinery Equipment, Beijing 100089, China*
[3]*National Special Superfine Powder Engineering Research Center, Nanjing University of Science and Technology, Nanjing 210094, China*

Received 10 February 2011; accepted 1 October 2011
DOI 10.1002/app.36258
Published online 17 January 2012 in Wiley Online Library (wileyonlinelibrary.com).

ABSTRACT: The synthesis of magnetic protein nanospheres via a modified sonochemical route was described. The effects of experimental parameters, such as bovine serum albumin dosage, ferrofluid concentration, ferrofluid dosage, ultrasonic power and time on the morphology, and dispersibility of magnetic protein nanospheres, were investigated. The final magnetic protein nanospheres were characterized by Fourier-transform infrared spectroscopy, transmission electron microscopy, scanning electron microscopy, thermogravimetric analysis, and vibrating sample magnetometer. The results showed that the superparamagnetic protein nanopsheres had small particle size of 100 nm, high saturation magnetization, high magnetite content, and abundant functional groups. These biocompatible protein nanospheres have biomedical applications. © 2012 Wiley Periodicals, Inc. J Appl Polym Sci 125: 1833–1840, 2012

Key words: biocompatibility; magnetic polymer; morphology; nanocomposites; TEM

INTRODUCTION

Magnetic protein microspheres have a wide range of biomedical applications, such as optical coherence tomography, fluoroimmunoassay, cell separation, and targeted drug delivery.[1–4] Magnetic protein microspheres are considered as promising materials for biomedical application, due to their biocompatibility, nontoxicity, high stability, and magnetic responsivity.[5] So far, many processes have been developed for preparing magnetic protein microspheres, including covalent immobilization, heat denaturation, and sonochemical method.[6–8] Among the various routes, sonochemical method has attracted considerable attention due to its convenient processing, simple experimental setup, significant saving in time, and excellent products.[9] Sonochemical synthesis of magnetic protein microspheres has also been reported in the past. Bunker et al. synthesized protein–metal oxide nanostructures with different morphology by the sonochemical method.[8] Avivi et al. prepared magnetic proteinaceous microspheres from bovine serum albumin (BSA) and iron compounds.[10] Han et al. developed a new targeted delivery system by depositing magnetic nanoparticles on protein containers, which were prepared by sonicating oil in a protein solution.[11]

According to previous works, the control of morphology of magnetic microspheres leads to a significant effect on the chemical and physical properties.[12,13] In this study, we focused on the manipulation of the morphology and encapsulation of magnetic protein nanospheres. Meanwhile, the possible mechanism of how the reaction parameters affected the formation of products was also investigated.

EXPERIMENTAL

Materials

The cyclohexane-based Fe_3O_4 ferrofluids were self-prepared using the modified chemical coprecipitation.[14] BSA was of analytical grade and supplied by Shanghai Huixin Biochemical Reagent. All the other reagents were obtained from commercial source and used without further purification.

Correspondence to: X. Zhang (xixi@jit.edu.cn).
Contract grant sponsor: National Natural Science Foundation of China; contract grant number: 50972060.
Contract grant sponsor: Cooperation Project Fund with Nanjing University of Science and Technology; contract grant number: jit-x-201005.
Contract grant sponsor: Natural Science Fund for Colleges and Universities in Jiangsu Province; contract grant number: 10kjd430008.
Contract grant sponsor: Jinling Institute of Technology (Dr Start-up Fund Research); contract grant number: jit-b-201013.

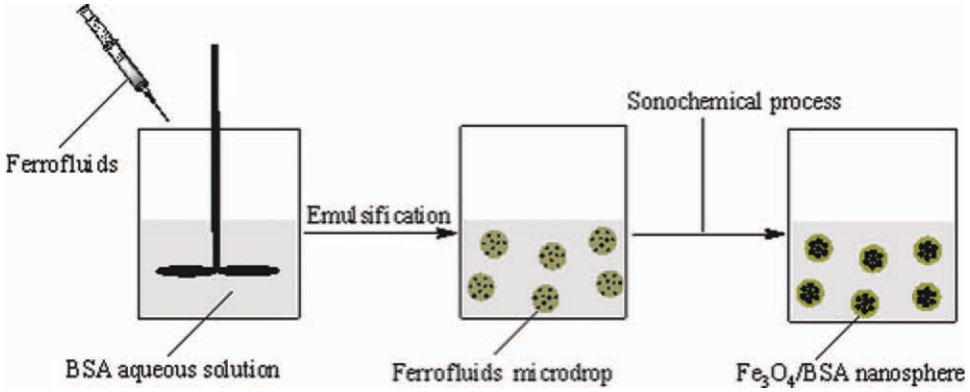

Figure 1 Schematic diagram of Fe_3O_4/BSA nanospheres prepared by the sonochemical method. [Color figure can be viewed in the online issue, which is available at wileyonlinelibrary.com.]

Preparation of Fe_3O_4/BSA nanospheres

Figure 1 schematically illustrates the fabrication procedure of Fe_3O_4/BSA nanospheres. First, appropriate amount of BSA was dissolved in 50-mL distilled water. Then, cyclohexane-based Fe_3O_4 ferrofluids was dropwise added to BSA solution and stirred for pre-emulsification. Second, the emulsion was subjected to sonication in an ice-cooled bath with JY92-II sonifier. Finally, the obtained water-soluble protein nanospheres were collected using magnet. Then, it was washed with ethanol and distilled water for removing the unreacted BSA. The reaction conditions for samples by the above-mentioned sonochemical method are outlined in Table I.

By taking sample-1 and sample-2 as example, we specified how to prepare Fe_3O_4/BSA nanospheres. The procedure preparing sample involved (a) dissolving 2.5 or 1 g BSA in 50-mL distilled water, (b) adding some ferrofluid to the BSA solution and stirring for pre-emulsification, (c) sonicating the emulsion with a sonifier, and (d) collecting the obtained samples with magnet and washing them.

Characterization

Fourier-transform infrared spectroscopy spectrum of KBr powder pressed pellets was recoded on a Bruker Vector 22 spectrometer. Transmission electron microscopy (TEM) images were recorded on a Tecnai 12 transmission electron microscope. Particles were coated with a thin gold layer before measuring by field emission scanning electron microscopy (FE-SEM, ModelS-4800). The America TA SDT Q600 thermal analyzer was used at a heating rate of 20°C/min in N_2 over the range 50–900°C with Al_2O_3 as reference. The magnetic properties of sample were detected at room temperature using vibrating sample magnetometer (VSM; Lake Shore 7410).

RESULTS AND DISCUSSION

FTIR analysis

Figure 2 shows the FTIR spectrum of magnetic nanospheres, which are used to ensure the presence of BSA protein. The characteristic absorption bands of Fe_3O_4 appear at 580 cm^{-1}.[15] The peaks at 3432 and

TABLE I
Samples Prepared with Different Reaction Conditions and Their Morphology

Samples	BSA dosage (g)	Ferrofluid concentration (wt %)	Ferrofluid dosage (g)	Ultrasonic power (w)	Ultrasonic time (min)	Morphology
Sample-1	2.5	20, 50	0.5–5	200–800	10–25	Irregular
Sample-2	1	20, 50	0.5–5	200–800	10–25	Spherical
Sample-3	1	50	0.5–5	200–800	10–25	Incomplete encapsulation
Sample-4	1	20	0.5–5	200–800	10–25	Complete encapsulation
Sample-5	1	20	0.5	200–800	10–25	Conglutination
Sample-6	1	20	2	200–800	10–25	Dispersed structure
Sample-7	1	20	5	200–800	10–25	Bad formability
Sample-8	1	20	1	200	10–25	Agglomeration
Sample-9	1	20	1	600	10–25	Bulk agglomerates
Sample-10	1	20	1	800	10–25	Incomplete encapsulation
Sample-11	1	20	1	300	10	Bad formability
Sample-12	1	20	1	300	20	Bulk agglomerates
Sample-13	1	20	1	300	25	Large agglomerates
Sample-14	1	20	1	300	15	Core-shell nanospheres

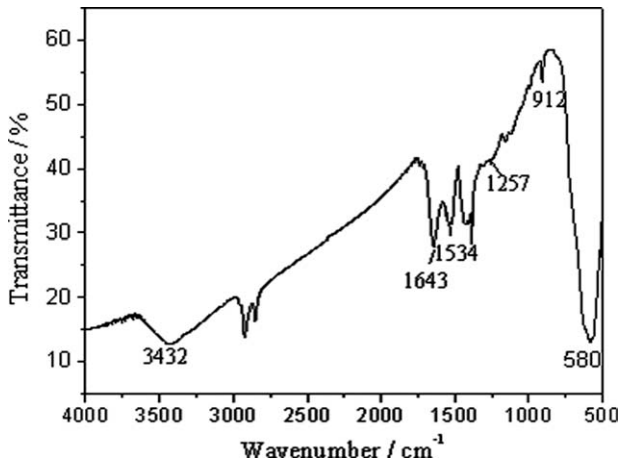

Figure 2 FTIR spectrum of Fe_3O_4/BSA magnetic nanospheres.

912 cm^{-1} are assigned to the stretching and wagging vibration of N—H bond, respectively. The peaks at 1643 cm^{-1} can be referred to the stretching vibration of C=O bond. Furthermore, the peaks at 1534 and 1257 cm^{-1} are attributed to the coupling vibration of N—H and C—N bonds. These results indicate that the functional groups (—CO—NH—) are located on the surface of magnetic nanospheres. So, it is confirmed that the shell of magnetic nanosphere is BSA.

Electron microscopy analysis

Effect of the BSA dosage

Figure 3 shows the TEM images of Fe_3O_4/BSA nanospheres prepared with different BSA dosage. Figure 3(a) reveals that the magnetic nanospheres are irregular by adding 2.5 g BSA. From Figure 3(b), we could see that the nanospheres are regular sphericity, but the particle size uniformity decreases. It could be attributed that 2.5 g BSA is over the limit value. Excessive BSA would prevent the volatilization of cyclohexane and absorb the free radical, leading to the difficulty in the formation of spherical shell. Therefore, based on the experimental results, the optimal BSA dosage is 1 g.

Further, we investigate the effect of BSA in detail. In the pre-emulsification, some BSA act as surfactant-like and form a modified layer around the ferrofluid droplet by physical adsorption. Additionally, in the sonochemical process, the BSA molecules are not significantly denatured and are held together to form inner shell by the disulfide bonds. Thus, the compact BSA-modified layers can not only enhance the stability of droplets to prevent the growth but also prevent the outflow of Fe_3O_4 nanoparticles to realize the complete encapsulation.

Effect of the ferrofluid concentration

The effect of ferrofluid concentration on Fe_3O_4/BSA nanospheres was also investigated. Comparing Figure 4(a) with (b), at the same reaction condition, with further increase in the ferrofluid concentration to 50 wt %, the obtained products were found to have incomplete encapsulation and agglomeration. The excessive ferrofluid concentration would lead to the difficulty in the dissolution of ferrofluid and the formation of ferrofluid microdroplet.[16] Meanwhile, less cyclohexane was easy to volatilize completely before the formation of shell, and the products were destroyed without the protection of shell. Thereby, the excessive ferrofluid concentration would result in the incomplete encapsulation of products, and the ferrofluid concentration was fixed on 20 wt %.

Effect of the ferrofluid dosage

The total content of ferrofluid is also an important reaction condition except its concentration. TEM images of Fe_3O_4/BSA nanospheres prepared with

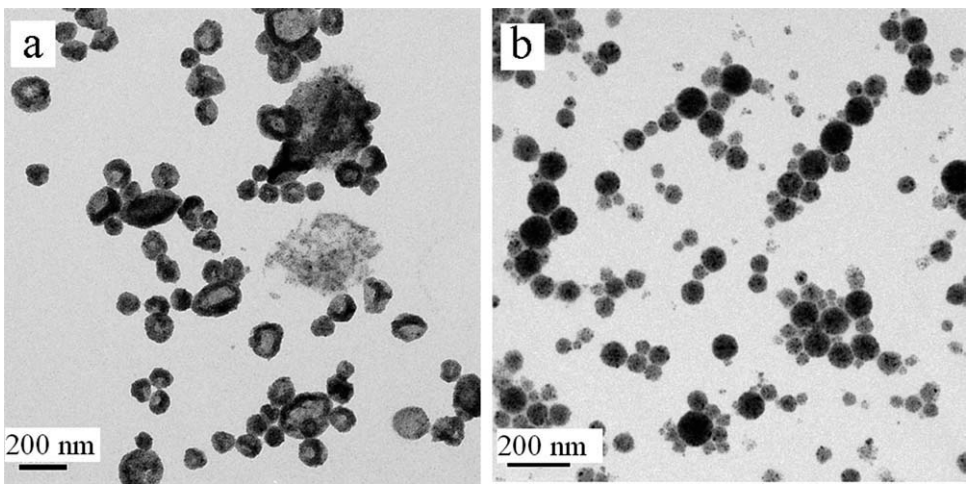

Figure 3 TEM images of Fe_3O_4/BSA nanospheres prepared with different amounts of BSA: (a) 2.5 g and (b) 1 g.

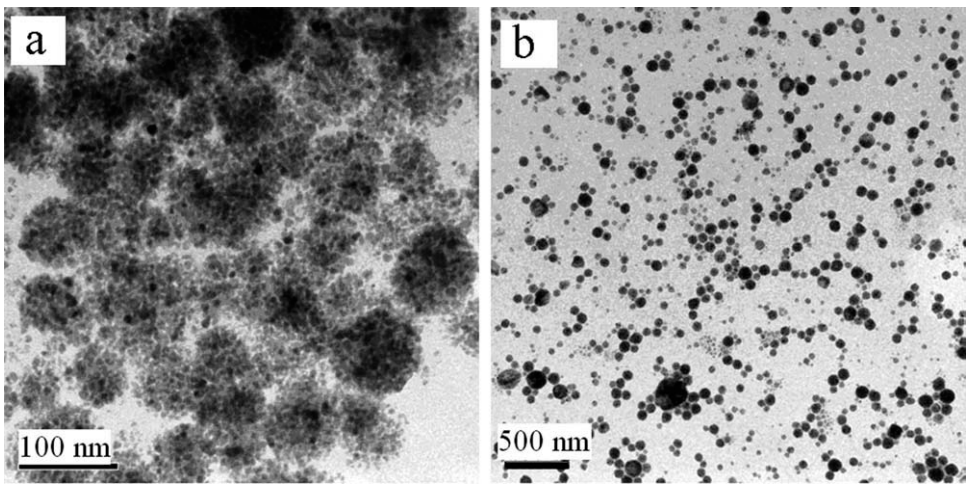

Figure 4 TEM images of Fe_3O_4/BSA nanospheres prepared with different ferrofluid concentrations: (a) 50 wt % and (b) 20 wt %.

different contents of ferrofluid are shown in Figure 5. From Figure 5(a), by adding 0.5 g ferrofluid, the prepared nanospheres exhibit core-shell structure but conglutination. Comparing Figure 5(a) with (b), by adding 2 g ferrofluid, the prepared nanospheres present dispersed structure and have thin BSA shell. Further increasing the ferrofluid dosage to 5 g [Fig. 5(c)], the obtained products have irregular morphology and agglomeration. Consequently, when the ferrofluid concentration is fixed on 20 wt %, the optimal ferrofluid dosage is 1 g.

Effect of the ultrasonic power

Figure 6 reveals the TEM images of Fe_3O_4/BSA nanospheres prepared at different ultrasonic powers.

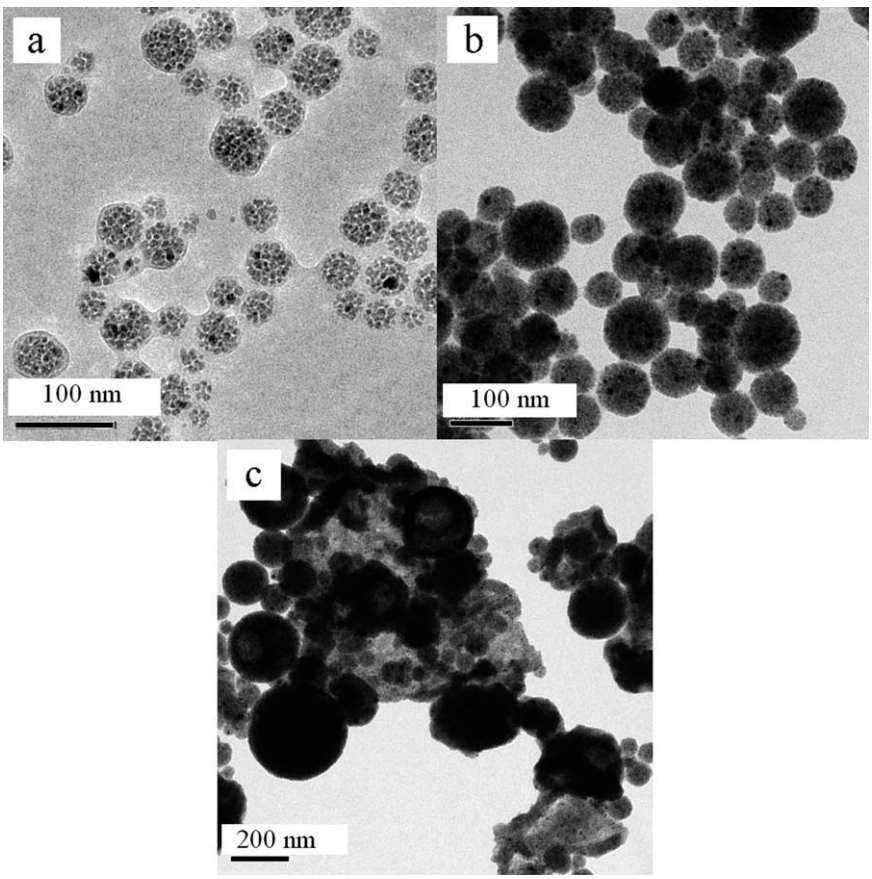

Figure 5 TEM images of Fe_3O_4/BSA nanospheres prepared with different contents of ferrofluids: (a) 0.5 g, (b) 2 g, and (c) 5 g.

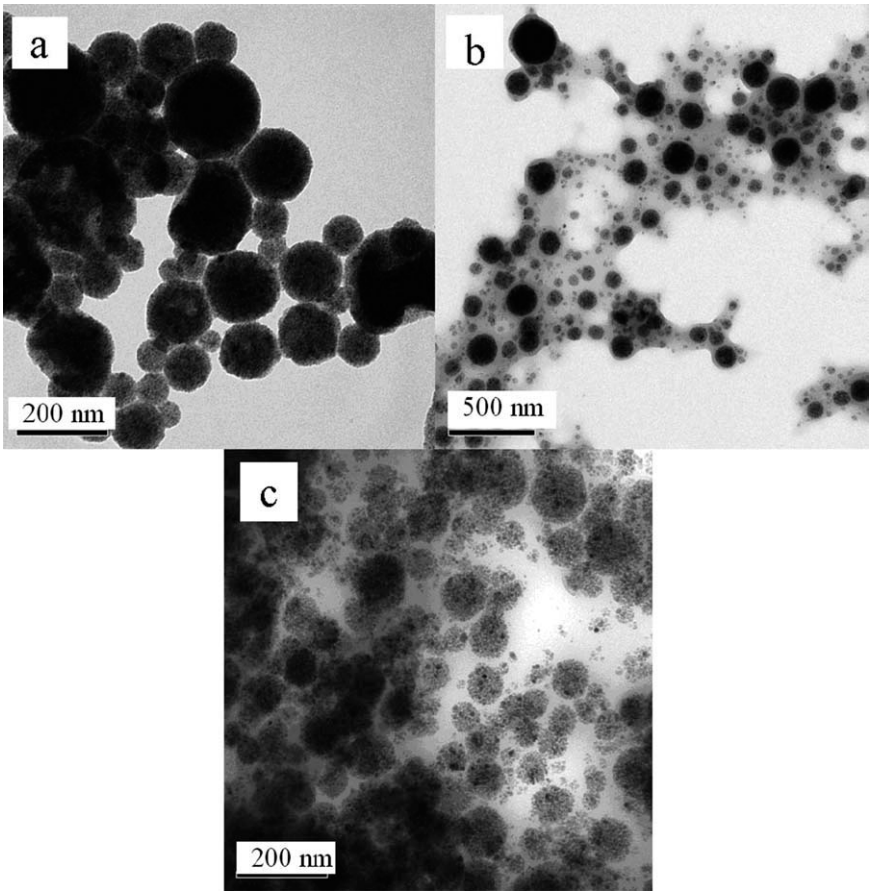

Figure 6 TEM images of Fe_3O_4/BSA nanospheres prepared at different ultrasonic power: (a) 200 w, (b) 600 w, and (c) 800 w.

From Figure 6(a), when the ultrasonic power is 200 w, the obtained products have bad sphericity and heavy agglomeration. Figure 6(b) shows that when the ultrasonic power is 600 w, the obtained products are bulk aggregates in which BSA nanospheres are embedded. It is attributed that abundant radicals are produced in short time, the polymerization reaction occurs rapidly and generates the BSA-encapsulated nanospheres. However, most of BSA proteins are denatured due to high heat produced in short time, thereby forming the bulk aggregates. From Figure 6(c), further increasing the ultrasonic power to 800 w, the intensive ultrasonic not only produces bulk aggregates but also destroys the embedding BSA nanospheres. On the basis of these results, the optimal ultrasonic power is fixed on 300 w.

Effect of the ultrasonic time

The effect of ultrasonic time on Fe_3O_4/BSA nanospheres was also investigated. From Figure 7(a), when the ultrasonic time was 10 min, the obtained products were found to have incomplete structure and size ununiformity. When the ultrasonic time reached 20 min [Fig. 7(b)], the obtained products were bulk denatured aggregates due to overreaction and high heat. From Figure 7(c), further increasing the ultrasonic time to 25 min, the obtained products formed larger bulk by connecting the aggregates, and BSA nanospheres were embedded in bulk aggregates. It can be concluded that the moderate denaturation of BSA was favorable for the formation of shell, because the BSA were held together to form the shell by the disulfide bonds via interprotein cysteine oxidation.[9] However, the excessive denaturation of BSA was disadvantageous for the formation of nanospheres, because it would result in the formation of bulk aggregates. According to these results, the optimal ultrasonic time was 15 min.

Effect of the pre-emulsification

The effect of pre-emulsification on Fe_3O_4/BSA nanospheres was also investigated. From Figure 8(a), without the pre-emulsification, the prepared products exhibited the size ununiformity and agglomeration. It can be ascribed that without the pre-emulsification, the polymerization started before the end of ultrasonic emulsification, which resulted in the agglomeration and size ununiformity of products. Comparing Figure 8(a) with (b), the obtained nanospheres with

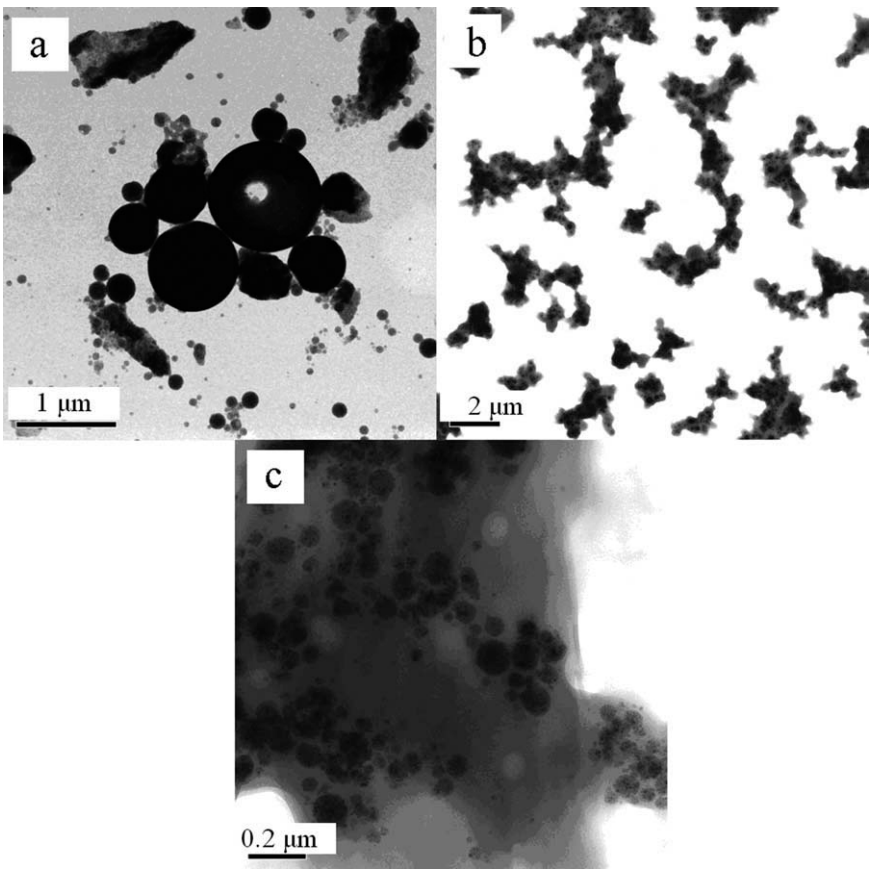

Figure 7 TEM images of Fe_3O_4/BSA nanospheres prepared at different ultrasonic time: (a) 10 min, (b) 20 min, and (c) 25 min.

the pre-emulsification had smaller particle size, better size uniformity, and dispersibility.

TEM and SEM of Fe_3O_4/BSA nanospheres

As shown in Table I, sample-14 was prepared on the basis of the optimal reaction parameters. Figure 9 showed the TEM and SEM images of sample-14 obtained under the optimal condition. From Figure 9(a), the Fe_3O_4/BSA nanospheres had core-shell structure, small particle size of 100 nm, good dispersibility and sphericity. From Figure 9(b), we could see the three-dimensional effect of magnetic protein nanospheres.

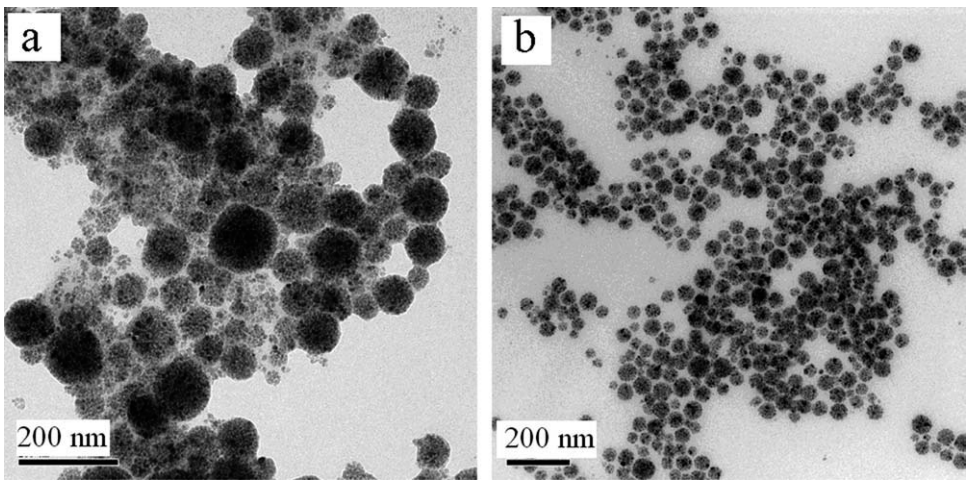

Figure 8 TEM images of Fe_3O_4/BSA nanospheres prepared: (a) without and (b) with pre-emulsification.

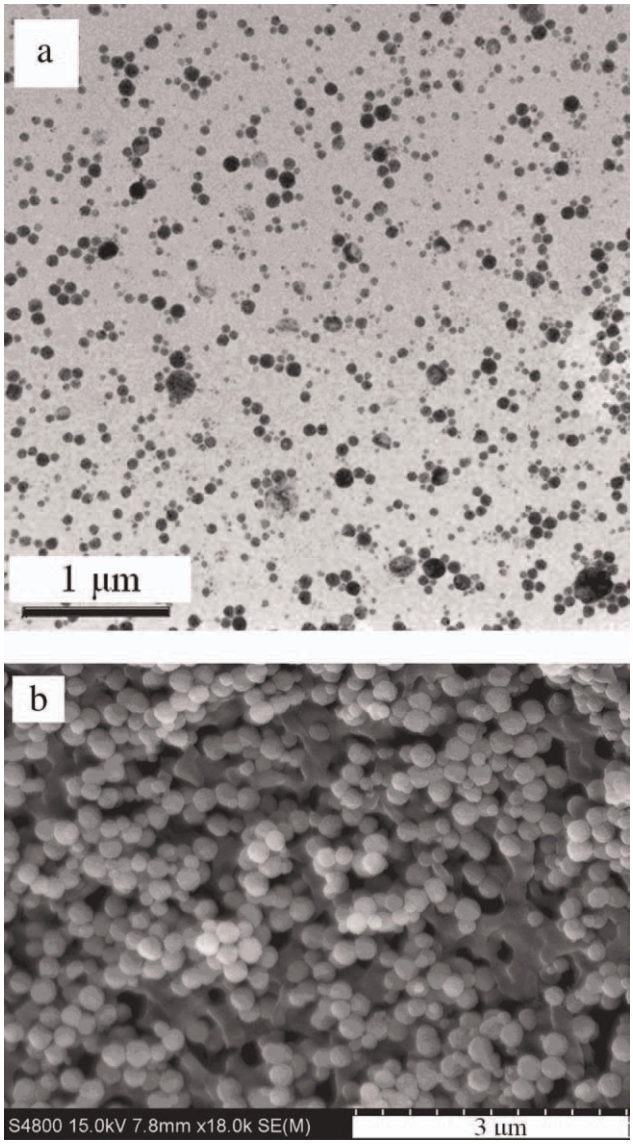

Figure 9 (a) TEM and (b) SEM images of sample-14.

TG and VSM analysis

The thermal stability of Fe_3O_4/BSA nanospheres was evaluated by TGA. Figure 10 showed the TGA curve of sample-14. The weight loss before 150°C was because of desorption of water adsorbed onto the sample. When being heated to 200°C, the weight loss velocity of sample began to accelerate, thanks to the decomposition of protein. It was comfirmed that the thermal stability of nanospheres was enhanced due to the crosslinking of BSA molecules. At 780°C, the organics were completely decomposed, leaving only magnetite. For that reason the curve tended to flat. The total weight loss of nanospheres was 42.4% in all, which indicated that the protein spheres contained 57.6% of magnetite nanoparticles. The high magnetite content of sample-14 indicated that they had a strong magnetic sensitivity under an outer magnetic field.

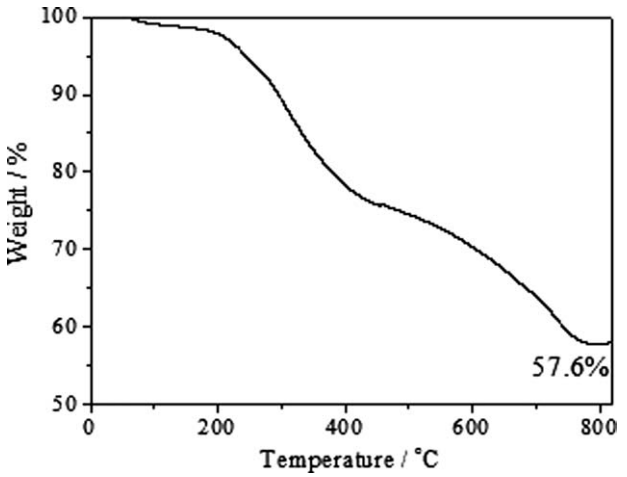

Figure 10 TGA curve of sample-14.

Furthermore, the magnetization curve of nanospheres was characterized by VSM. The product exhibited apparent superparamagnetism without any hysteresis.[17] The superparamagnetic behavior was also reflected in the low residual magnetization (M_r) and coercivity (H_c) values. Figure 11 showed that the saturation magnetization (M_s) of sample-14 was 38.5 emu/g. It could be seen that Fe_3O_4/BSA nanospheres with high saturation magnetization could be synthesized by controlling the reaction conditions.

The formation mechanism of Fe_3O_4/BSA nanospheres

The possible formation process of Fe_3O_4/BSA magnetic nanospheres is discussed in detail. First, in the pre-emulsification, the cyclohexane-based Fe_3O_4 ferrofluids have good dissolubility in BSA solution by physical absorption. Second, in the sonochemical process, the BSA molecules are not significantly denatured and are held together to form inner shell by the sonochemical formation of disulfide bonds.[18]

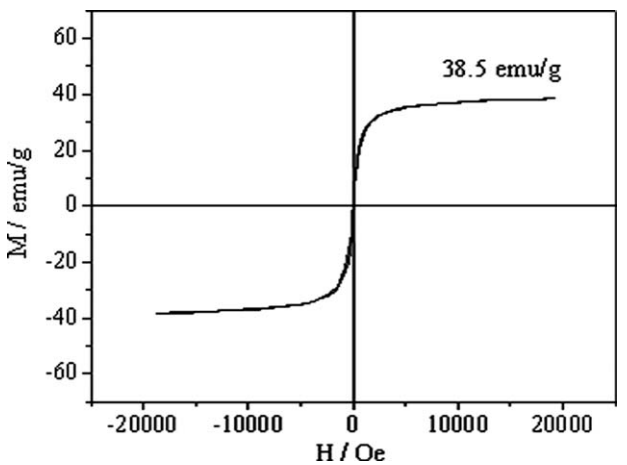

Figure 11 Magnetization curve of sample-14.

Then BSA layers continually construct outside of the ferrofluid, meanwhile, the toxic solvent cyclohexane evaporates rapidly due to the heat generated by ultrasonication, which turns the encapsulated ferrofluid microdroplets into solid core of Fe_3O_4 nanoparticles. Finally, the core/shell Fe_3O_4/BSA nanopheres with nontoxicity are obtained.

CONCLUSIONS

In summary, Fe_3O_4/BSA nanospheres have been prepared by a modified sonochemical route. We successfully manipulate the morphology and encapsulation of magnetic protein nanospheres by adjusting the reaction parameters and discuss the possible formation mechanism of fine Fe_3O_4/BSA nanospheres in detail. The procedure is facile and well-controlled for the synthesis of Fe_3O_4/BSA nanospheres and could be potentially applied to the preparation of other magnetic protein nanospheres. Such magnetic Fe_3O_4/BSA nanospheres are promising materials for biomedical application. Besides, further works are now in progress in our laboratory.

References

1. Nguyen, F. T.; Dibbern, E. M.; Chaney, E. J.; Oldenburg, A. L.; Suslick, K. S.; Boppart, S. A. Proc SPIE 2008, 6867, 68670F-1.
2. Wang, J. Y.; Wang, X. Q.; Ren, L.; Wang, Q.; Li, L.; Liu, W. M.; Wan, Z. F.; Yang, L. Y.; Sun, P.; Ren, L. L.; Lin, M. L.; Wu, H.; Wang, J. F.; Zhang, L. Anal Chem 2009, 81, 6210.
3. Widder, K. J.; Senvei, A. E.; Ovadia, H.; Paterson, P. Y. Clin Immunol Immunopathol 1979, 14, 395.
4. Timko, M.; Koneracká, M.; Kopčanský, P.; Ramchand, C. N.; Vékas, L.; Bica, D. Czech J Phys 2004, 54, D599.
5. Avivi, S.; Nitzan, Y.; Dror, R.; Gedanken, A. J Am Chem Soc 2003, 125, 15712.
6. Guo, N.; Wu, D. C.; Pan, X. H.; Lu, M. L. J Appl Polym Sci 2009, 112, 2383.
7. Teresa, W.; Chan, M. D.; Crispin, E.; Liberti, P.; Andrew, S. O.; Herbert, Y.; Kressel, M. D. Invest Radiol 1992, 27, 443.
8. Bunker, C. E.; Novak, K. C.; Guliants, E. A.; Harruff, B. A.; Meziani, M. J.; Lin, Y.; Sun, Y. P. Langmuir 2007, 23, 10342.
9. Suslick, K. S.; Grinstaff, M. W.; Kolbeck, K. J.; Wong, M. Ultrason Sonochem 1994, 1, S65.
10. Avivi, S.; Felner, I.; Novik, I.; Gedanken, A. Biochim Biophys Acta 2001, 1527, 123.
11. Han, Y. S.; Radziuk, D.; Shchukin, D.; Moehwald, H. Macromol Rapid Commun 2008, 29, 1203.
12. Lu, S. L.; Cheng, G. X.; Pang, X. S. J Appl Polym Sci 2006, 100, 684.
13. Xu, Y. W.; Xu, H.; Gu, H. C. J Polym Sci Part A: Polym Chem 2010, 48, 2284.
14. Zheng, W. M.; Gao, F.; Gu, H. C. J Magn Magn Mater 2005, 288, 403.
15. Luo, Y. L.; Fan, L. H.; Xu, F.; Chen, Y. S.; Zhang, C. H.; Wei, Q. B. Mater Chem Phys 2010, 120, 590.
16. Zhang, X. J.; Jiang, W.; Ye, Y. F.; Feng, Z. Q.; Sun, Z. D.; Li, F. S.; Hao, L. Y.; Chu, J. J. J Magn Magn Mater 2011, 323, 1440.
17. Chen, Z. M.; Jiao, Z.; Li, Z. Q. J Appl Polym Sci 2008, 110, 1664.
18. Toublan, F. J.; Boppart, S.; Suslick, K. S. J Am Chem Soc 2006, 128, 3472.